Complementary Use of Airborne LiDAR and Terrestrial Laser Scanner to Assess Above Ground Biomass/Carbon in Ayer Hitam Tropical Rain Forest

Cora Jane C. Lawas[1], Yousif Ali Hussin[2], Evert Henk Kloosterman[3]

[1] Central Visayas Studies Center-University of the Philippines Cebu, 6000

Lahug Cebu City, Philippines

[2,3] Faculty of Geo-Information Science and Earth Observation, University of Twente,

7500 AE Enschede, The Netherlands

Email: cclawas1@up.edu.ph, y.a.hussin@utwente.nl, e.h.kloosterman@utwente.nl

Abstract: This study aimed to develop a method of assessing the AGB/carbon stock of a tropical lowland rainforest with a vertically complex structure. The method utilizes the complementary strengths of airborne LiDAR and terrestrial laser scanning system to assess the upper and lower canopies of the forest to achieve reasonable results. The method was implemented in Ayer Hitam Forest Reserve in Malaysia. The upper canopy layer was assessed by generating tree parameters using airborne LiDAR to obtain height from CHM and segmenting the Orthophoto to obtain CPA. DBH was modelled through multiple regression using the derived parameters as independent variables and the field DBH as the dependent variable. The modelled DBH achieved an R^2 value of 0.90 and RMSE of 0.02 cm for the 16 plots. To estimate the AGB an allometric equation was applied to the modelled DBH together with LIDAR derived height. The modelled AGB was validated using the field DBH and LiDAR derived height. The derived model has an R^2 of 0.98 and RMSE of 69.44 Kg for the 16 plots.

The lower canopy layer was assessed using the registered scene from the TLS. This is to complement the trees that were not identified from the upper canopy layer. Scanned trees in the plot were extracted. Then DBH and height parameters were measured using RiSCAN Pro software interface. These parameters were then used for the allometric equation to estimate the AGB for the lower canopy. The correlation of the TLS measured DBH and field measured DBH was established and achieved an R^2 value of 0.99 and RMSE of 1.03 cm. The modelled AGB was estimated using the TLS measured height and DBH by applying the allometric equation. The model was validated using the field measured DBH and TLS derived height. The result was a model with an average R^2 value of 0.99 and RMSE of 19.23 Kg for the 16 plots. The derived AGB from the upper and lower canopies were combined. The accuracy of the complementary method of deriving the estimated AGB from the two sensors was assessed by obtaining the R^2 and RMSE of the two sensors. The achieved R^2 and RMSE is 0.98 and 188.35 kg respectively for the 16 plots.

The results in this study presented a potential method of addressing the need to provide accurate AGB/carbon assessment for a complex multi-layered tropical rain forest.

Keywords: Airborne LiDAR, Terrestrial laser scanner (TLS), Segment, AGB, allometric equation.

1. Introduction

The ecosystem function of forests to store carbon play an important role in the global agenda of climate change. Carbon stored in forests serve as an important natural brake on climate change (Gibbs, et al 2007). The ecosystem disturbance of forest due to deforestation and degradation convert forests into carbon sources instead of sinks. The mitigating instrument implemented to address the emissions from deforestation and forest degradation in developing countries is reducing emissions (REDD+), plus stands for conserving and enhancing forest stocks and sustainable management of forests (Corbera & Schroeder, 2011, Pistorius, 2012).

The objectives of the REDD+ is the sustainable and time bound reduction of forest related greenhouse gas emissions. The program requires functional and sustainable national monitoring and verification (MRV) systems. Estimating greenhouse gas (GHG) emissions according to the United Nations Framework Convention on Climate Change (UNFCC) must be based on the guidelines set by the Intergovernmental Panel on Climate Change (IPCC). This is based on the use of remote sensing techniques and ground based forest carbon inventory (UN-REDD programme, 2015). The applicability of the method however is dependent on the specific type of forest, the complexity of the geographical location and conditions of the forest (Ediriweera, et al., 2014;Tonolli et al., 2011).

For tropical lowland rainforest like Ayer Hitam Forest Reserve (AHFR) this poses a challenge. The structure of this type of forest is stratified according to different layers (Walter et al., 1973). These are classified as emergent, canopy, understory and forest floor (Figure 1). The distinct stratification is due to the optimal conditions for rapid plant growth and competition. Carbon assessment therefore must account for the trees in all the canopy layers.

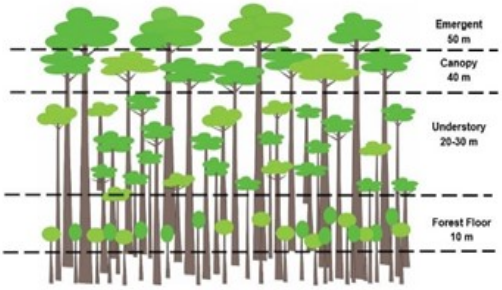

Figure 1. Structure of a tropical lowland tropical rain forest.

Under the REDD+ framework monetary incentives can only be provided for carbon reduction initiatives if above ground biomass (AGB) of this type of forest will be accurately accounted through remote sensing methods. However, as reviewed by Koch (2010) there is very limited information on LiDAR derived data for biomass mapping in the tropics. Moreover as pointed out by Hirata et al., (2012) there is a need for separate biomass assessment methods to appropriately assess multi-layered tropical forests. A new approach of accurately assessing the AGB of a vertically complex tropical rainforest has to be developed in answer to the REDD+ requirement. The overall concept of this study is the synergistic use of airborne LiDAR with an Orthophoto for the assessment of the emergent and canopy layers of the forest. Complementary to this, is the use of a terrestrial laser scanner for the assessment of the understory layer of the forest. Due to the distinct vertical structure of this type of forest its assessment would require both airborne and terrestrial remote sensors that can detect tree structural parameters across different layers. These laser sensors have their inherent strength and weakness when applied to temperate forests (Van Leeuwen et al., 2011).

Airborne laser sensors have limitations to characterize vegetation structure in the lower canopy. Whereas terrestrial laser sensors are biased towards lower parts of the canopy (Hilker et al., 2010). Studies on the integration of these technologies in temperate forests enhances the detail of structural information (Chasmer et al.,2006; Hilker et al., 2010). The complementary application of these remote sensing technologies in a lowland tropical rainforest as of this writing has yet to be tested. This innovative concept was studied if it has the potential to provide a robust information on the accurate assessment of AGB for a vertically complex tropical rain forest for the application of REDD+ program.

2. Materials and Methods

2.1 Study Area

Ayer Hitam tropical rain Forest Reserve (AHFR) is a logged over lowland mixed-dipterocarp forest in the State of Selangor, Malaysia which covers an area of 1,248 hectares (Ibrahim, 1999) Figure 2. The forest is one of the three remaining lowland dipterocarp forests in the Klang Valley. It has been isolated from the neigh boring forests due to the residential and other economic development that surrounds the whole forested area (Nurul Shida et al., 2014). AHFR's location is 3° 01' N and 101° 39' E shown in Figure 1. The forest reserve has distinct topographical characteristics namely ridge, hillside and valley. The elevation ranges from 15m to 233m. The slope of the terrain is 34º. The temperature ranges from 22 to 32 ºC, the average relative humidity is 83% and the annual rainfall is 2,178 mm. The forest reserve has been leased to the University of Putra in Malaysia (UPM) for 80 years for education, research and extension purposes (Ibrahim, 1999).

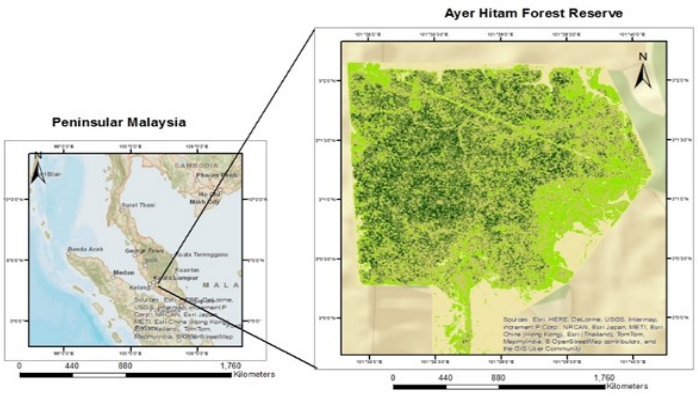

Figure 2. Location map of Ayer Hitam Forest Reserve.

2.2 Biometric Data Acquisition

The actual field work was done from Sept. 29 to Oct. 12, 2015 to collect the ground truth primary data of the study area. Using Arcmap software World View3 image of the study area was georeferenced to WGS 84 Zone 47N. Gridlines were drawn in the final map layout and potential plots were plotted to ensure that a 50m distance between plots. The map with the potential plots were then uploaded into the Google NexusTablet and used for navigation during field data collection. Circular plots of 13m depending on the slope were demarcated to obtain a 500 m^2 area plot. Within the demarcated plot DBH of trees having a 10 cm or greater DBH were measured. To obtain uniform DBH from the ground a 1.3 m measured stick was used as standard measuring guide above the buttress of each tree (Maas et al., 2008). Trees with less than 10 cm DBH were not considered because they do not contribute much to the carbon of the forest (Brown, 1999). Height of these measured trees were measured using Leica DISTO D510 Laser Ranger.

2.3 Airborne LiDAR and Orthophoto

Airborne LiDAR and Orthophoto data was provided by the University of Putra Malaysia. This was acquired on July 23, 2013. These data sets were used to assess the upper tree canopy. This was acquired using LiteMapper 5600 a waveform-digitizing LiDAR for terrain and vegetation mapping system. The point cloud density of the airborne LiDAR data is 5-6 points per m^2. This was flown over at 80–100 knot speed at 600m–1000 m above the ground. The manoeuvre would provide data with sufficient point densities and footprint sizes to achieve at least 3 points/m^2. The laser footprint covered targeted areas with an average overlapping of 50% between adjacent flight lines. The maximum scan was set at 11°; pulses transmitted at scan angles that exceeded 8° were excluded from the final data in order to avoid low-quality data at the edge of strips (Hug et al., 2004).

The Orthophoto was taken simultaneously with the acquisition of the airborne LiDAR data. The spatial resolution of the image is 13 cm. The Lite Mapper-5600 system is equipped with an IGI DigiCAM to complement the LiDAR data. The coverage of the camera is the same swath as what the LiDAR system sees. This provided a high resolution imagery of the surface in true color to aid surface classification and to provide extra planimetric resolution (Hug et al., 2004). The calibrated lenses of the DigiCAM is tightly integrated with the LiteMapper-5600 and the IGI CCNS-4 flight management systems to facilitate reliable and easy operation. The camera is mounted together and boresighted with the laser scanner and the IMU to enable direct georeferencing of its images and automated ortho image generation using the DSM output of the LIDAR system (Hug et al., 2004).

2.4 Terrestrial Laser Scanner

Terrestrial laser scanner (TLS) data was acquired to assess the lower tree canopy. To ensure the quality of the acquired TLS point cloud data appropriate scanning steps were implemented. Namely, 1) plot preparation 2) tree tagging with numbers and 3) setting the multiple scan position. Multiple scanning was employed to produce better three dimensional scanned object. This is to ensure sufficient overlap of the scanned image and obtain better canopy height without compromising the quality of the point cloud data (Watt & Donoghue, 2005). Moreover, employing multiple scans will improve DBH measurement accuracy compared to single scans (Kankare et al., 2013). Retro-reflective objects (tie points) were established which serve as reference points for co-registration of the multiple scans. The TLS instrument RIEGL-VZ-400 was set on the tripod with the NIKON D610 camera mounted on top. Scan position was then fixed after which fine scanning of the reflectors was done to register the multiple scans.

2.5 Methods

Forest structural metrics for the different canopy layers of the forest were derived based on the data available. Thus, different methods were implemented both for the upper and lower canopy layers. Application of these methods were essential to derive AGB of the forest. For the upper canopy, CHM and DBH are requisites to model the DBH. Accuracy of the modelled DBH was assessed based on the field measured DBH. The modelled DBH and height from CHM was used to derive a modelled AGB using an allometric equation. Accuracy of the modelled AGB was validated based on the calculated AGB using the field measured DBH and CHM by applying the allometric equation. For the lower canopy height and DBH measurements were obtained from the TLS point cloud data. By applying the allometric equation a modelled AGB was obtained. Accuracy of the modelled AGB was validated by using the field measured DBH and TLS measured height by calculating the AGB using the allometric equation. Total modelled AGB from both upper and lower canopies were calculated and validated using the total AGB calculated from field measurements. The graphical presentation of the methods is shown in Figure 3.

2.5.1 Upper Canopy

Airborne LiDAR data processing

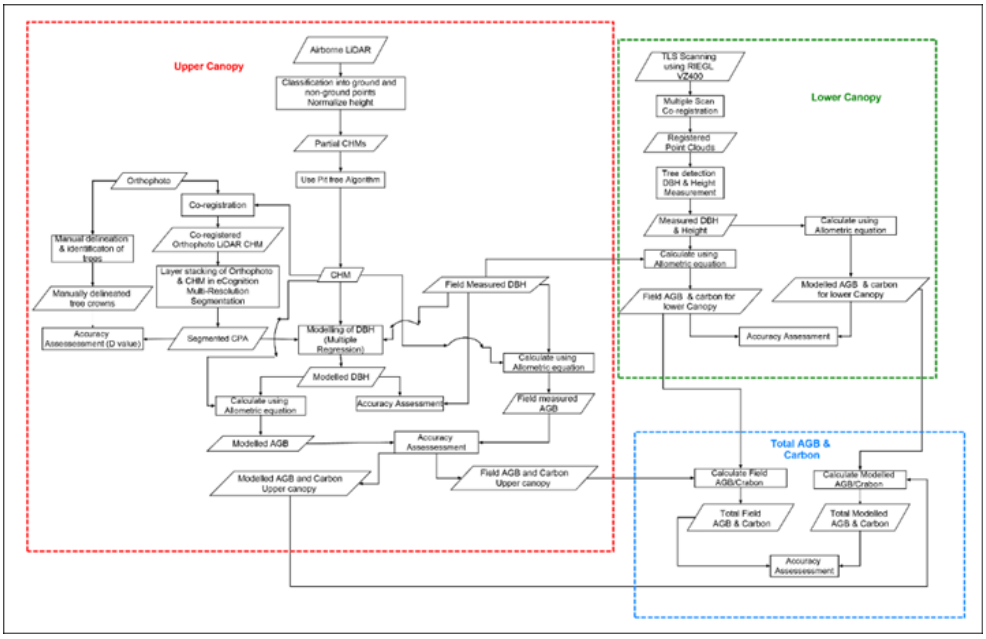

Figure 3. Methodology flow diagram.

Point cloud data obtained from airborne LiDAR was processed using LAS tools. Canopy height model (CHM) was generated by adopting the method of Khosravipour, et al., (2015) through the use of the pit free algorithm to create a pit free raster CHM. This is a direct processing of point cloud data into raster format. Using LAS tool lasground .las files were classified into ground and non-ground points. Height was normalized using the lasheight tool by replacing the elevation of each point with its height above the ground. Using the las2dem tool partial CHMs were generated then the pit free algorithm was used to convert the partial CHMs into a pit free raster CHM.

To note pit free CHM is a new method of creating CHMs (Ben-Arie, et al., 2009) and detailed comparison of the method had proven that it can provide better height metrics (Khosravipour, et al., 2015). Moreover, in this study adapting the method of generating better height metrics was essential because of the reliability of the primary ground height data that was acquired.

Orthophoto data processing

Tree crown segmentation utilizes the Orthophoto and the generated CHM. The two datasets were co-registered prior to its combination in eCognition. The two data sets were layer stacked in eCognition to fuse the two images. Multi-resolution segmentation process was applied to identify features using the scale and homogeneity parameters obtained from the spectral reflectance values from the Orthophoto and the elevation from the CHM (Suárez, et al., 2005). In this study the method has been adopted for this has been implemented for forest biomass estimation (Van Aardt et al., 2004). To determine the best fit scale, a scale of 10 was selected using the estimation scale parameter (ESP) tool (Drăgut et al., 2010). In the segmentation process the 10 scale parameter was used and for shape and compactness 0.8 and 0.6 values were used respectively.

Manual Identification and Delineation of Trees

To validate the CPA segmentation process manual tree identification and identification was done. This is a challenging task especially in thick canopied tropical forest. Handheld GPS system could not function properly under this environmental condition. The established plots were then reconstructed in the generated CHM and Orthophoto. Based on the acquired center plot location, and geotagged tree points near the center plot, individual trees were identified first using the images derived from the TLS. Its relative location was identified in RiSCAN software. Based on that information location of the tree was identified into the reconstructed plots in the Orthophoto using plot bearing as a guide to locate the tree. Using the height information of the tree from the TLS its location was further verified using the generated CHM. Tree crown delineation per plot was subsequently done using manually identified trees in the Orthophoto.

Segmentation Validation

Delineated tree crowns were assessed for segmentation accuracy and model validation. Tree crown segmentation accuracy employed visual and geometric techniques. Visual accuracy technique (Möller et al., 2007) assess the accuracy of the segmentation based on the relative area in reference to the manually digitized polygons. Geometric segmentation accuracy assess the extent of the segmented output with reference to a defined training set (Clinton, et al., 2010). The quality of the segmented output is defined in terms of over and under segmentation. Over segmentation and under segmentation as explained by Clinton, et al., (2010) based on Equations 1 and 2.

$$OverSegmentation_{ij} = 1 - \frac{area(x_i \cap y_j)}{Area(X_i)}, y_i \epsilon Y_i^* \quad \text{..... Equation 1}$$

$$UnderSegmentation_{ij} = 1 - \frac{area(x_i \cap y_j)}{Area(Y_i)}, y_i \epsilon Y_i^* \quad \text{..... Equation 2}$$

The goodness of fit is explained in terms of the distance index (D) which is the combination of over and under segmentation. The D value range is from 0 to 1, where 0 is a perfect match between the reference polygon and the segmented object and 1 is the minimum mismatch. The goodness of fit is calculated using Equation 3.

$$D_{ij} = \sqrt{\frac{Oversegmentation_{ij}^2 + Undersegmentation}{2}} \quad \text{..... Equation 3}$$

2.5.2 Lower Canopy

Terrestrial Laser Data Processing

The acquired point cloud data from the field was processed using RiSCANPRO software (RIEGL, 2015). It has a built in project data structure where acquired data is organized and stored. Using the software point cloud data was coarse registered by defining the tie points from the acquired scan position in two dimensional mode. The center scan position was used as the reference data set and the outer scan positions are the data set to be registered. The quality of the co-registered scans was improved through the application of multistation adjustment algorithm. This iteratively adjust the position and orientation of the scan position until the error is below the user defined threshold.

Plot and Individual Tree Extraction

The scanned point cloud data covers a large area and to separate the circular plots it was filtered. Plot measurement was based on recorded field data taking into consideration the slope correction of each plot. Area of interest was defined based on the points that were within plot distance using the range function of RiSCAN PRO. Individual trees were extracted from the plots through the selection of point clouds that resemble tree shape. Noise were manually removed. Recognized trees were sliced and saved as poly data for further tree parameter assessment.

Tree Height Measurement

Extracted tree poly data was retrieved and each individual tree was manually measured using the measuring tool of the software. The lowest (ground) and highest (tree top) points of each tree were located. The measurement tool read the x, y, & z values of measured points and the height was measured along the vertical axis between the lowest and highest points (Figure 4). The obtained height measurement was stored in a database format using Excel.

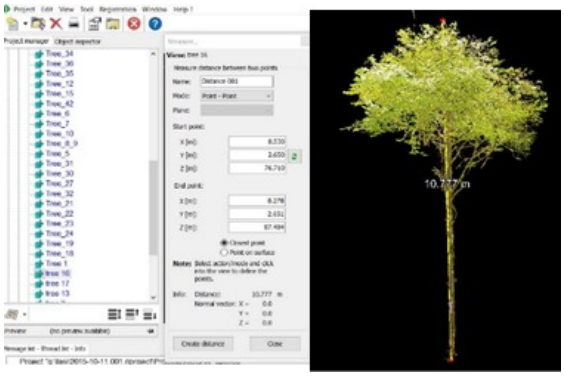

Figure 4. Tree height measurement of extracted trees.

DBH Measurement

DBH of the individual tree was determined at 1.3 m from the lowest point of the tree and the width of the stem of the tree of this height was measured on a point to point basis. The measurement tool then reads the x, y, & z values of the measured points and the width measurement is taken along the horizontal distance of the stem (Figure 5).

2.5.3 AGB and Carbon Stock Estimation

Using allometric equation is a common method of estimating forest biomass that can be used in large forest areas through non-destructive methods (Ketterings et al., 2001). The equation relates to tree structural parameters that can be repeatedly measured on the ground and can be used to estimate AGB. Selection of the appropriate allometric equation is essential for this determines the preciseness of AGB estimates. For a tropical forest like AHFR that stores highly diverse species of trees, local or geographical allometric equations may render inadequate estimates (Gibbs et al., 2007). This study adopted the generic equation (Equation 4) developed by Chave et al., (2014) because the equation is established based on a larger number of trees. Using the equation have the potential to increase the precision of AGB estimates. Precise estimation of AGB as a consequence will also provide precise carbon stock be estimation by multiplying the 50% factor (Drake et al., 2003)

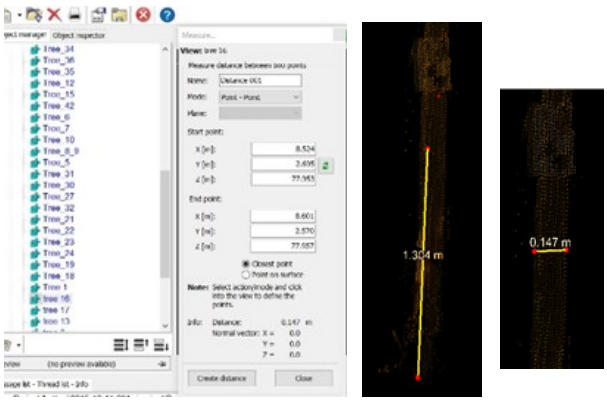

Figure 5. DBH measurement of extracted trees.

$$AGB_{est} = 0.0673\ x\ (\rho D^2 H)^{0.976} \quad \text{..... Equation 4}$$

Where,
AGB: Above ground biomass (Kg)
ρ: specific wood density
D: diameter at breast height
H: Height

2.6 Regression Analysis and Model Validation

Regression analysis is an established method for modelling the relationship between remotely sensed data and field measurements (Popescu, 2007; Lim et al., 2003). The method quantifies the relationship between the response variable and the explanatory variable. This type of statistical analysis is used in this study to establish relationships among the derived forestry parameters to account for the total AGB/carbon of the forest. To assess the upper canopy layer of the forest, multiple linear regression was used to model the relationship between the field measured DBH and the airborne LiDAR derived height and CPA derived from the Orthophoto to obtain a modelled DBH. While to assess the relationship between the modelled AGB and field measured AGB a linear regression was implemented. In assessing the AGB of the lower canopy layer of the forest, linear regression was used to establish the relationship between the modelled AGB using the TLS measured DBH and height and the field measured AGB using the field measured DBH and TLS height. Then to assess the relationship between the modelled total AGB and the total field AGB linear regression was used. To assess the performance of all modelled parameters the RMSE was calculated using the general equation (Equation 5).

$$RMSE = \sqrt{1/n \sum_{1}^{n} (P - O)^2} \quad \text{..... Equation 5}$$

Where,
P: Predicted
O: Observed
n: number of observations

3. Results

3.1 Field Data

Tree parameters namely DBH and crown diameter of the individual sampled trees were measured from the 16 field plots. The descriptive statistics of the sampled trees are shown in Table 1. The test for the normality of the field measured DBH and crown is shown in Table 2. Distribution and QQ plots of field DBH and tree crowns is shown in Figure in 6.

Table 1. Descriptive statistics of the sampled trees.

Statistic	Mean	Minimum	Standard Deviation	Number of trees
DBH (cm)	23.47	10	14.29	428
Crown Diameter (cm)	5.65	2.17	2.14	232

Table 2. Normality test of field measured DBH and crown.

	Kolmogorov-Smirmova			Shapiro-Wilk		
	Statistic	df	Sig.	Statistic	df	Sig.
DBH	0.173	0.428	0.000	0.789	0.428	0.000
Crown	0.076	232	0.002	0.956	232	0.000

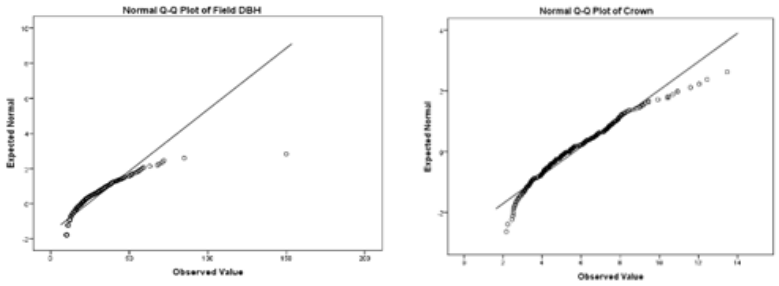

Figure 6. Distribution and QQ plots of field DBH and tree crowns.

3.2 Pit-free CHM from Airborne LiDAR Data

The CHM for the upper canopy layer of the forest was generated by classifying point cloud data into ground and non-ground points. The height was then normalized and partial CHMs were created (Figure 7). CHMs with pits have significant effects to height measurements. Application of the pit-free algorithm was essential to produce pit free CHMs (Figure 8).

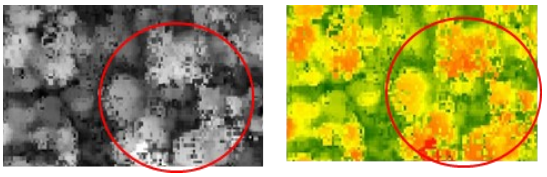

Figure 7. Two-Dimensional representation of partial CHMs with pits.

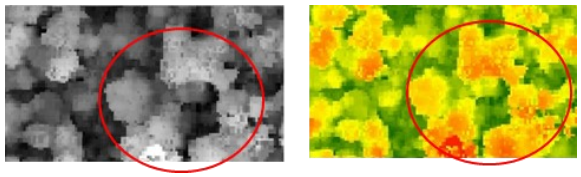

Figure 8. Pit-free CHMs

3.3 CPA segmentation accuracy assessment

Accuracy of segmented tree crowns was assessed based on D measures and 1:1 spatial correspondence for the 208 identified and manually delineated trees. The total 1:1 match is 160 out of the 208. This accounts to a 77% match. Over- and under segmentation at the scale of 10 is .09 and 0.03 respectively and D value of 0.25 (75%). This accounts to a total accuracy of 75% and a segmentation error of 25%. Table 3 show the accuracy assessment result.

Table 3. Segmentation accuracy assessment

Parameter	Total reference polygons	Total 1:1 match	Over segmentation	Under segmentation	D-value
1:1	208	160			
Goodness of fit			0.09	0.03	0.25
Total Accuracy		77%			75%

3.4 Registered Scans

Registration of 4 TLS scans using the point cloud data were aligned to the scanned positions to obtain a three-dimensional perspective of the scanned scene Figure 9. Creating the three-dimensional scene allowed the subsequent steps of identifying individual trees, tree extraction and tree parameter measurements (DBH and Height. Applying, this method and the subsequent multistation adjustment (MSA) obtained a standard deviation of 0.01-0.0234 cm of the point cloud data.

3.5 Individual Tree Detection

Individual tree detection was done by identifying point clouds that fit the shape of an individual tree. Identification was done through the tagged numbers to the individual trees in the plot. The process is based on the assumption that point clouds tend to aggregate near the circular points that is distributed through the vertical axis of some height which is separated from the adjacent stem. Tagged individual trees that were visibly identified were recognized as trees.

3.6 Individual Tree Extraction

Trees that were individually detected were extracted manually in RiSCAN PRO and stored as individual polydata. Figure 10 shows sample of individual trees extracted trees from RiSCAN PRO. From the extracted trees individual tree parameters such as DBH and height were measured using the measure interface of RiScan PRO. The obtained parameters were subsequently used for AGB modelling and estimation.

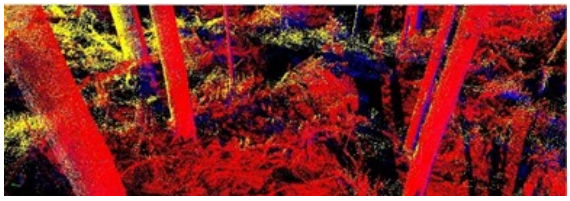

Figure 9. Three dimensional scene after registering the point cloud data.

Figure 10. Sample of extracted trees.

3.5 Plot selection for DBH and AGB analysis

Plot selection is essential for this study since it is necessary that the plots contain trees that complement from both sensors. There were only 16 plots identified viable for subsequent model analysis and AGB estimation. Other plots were excluded because trees were not detected from the CHM derived from airborne LiDAR and CPA from the Orthophoto. Moreover, not all trees that were detected were also extracted from TLS scanned plots. To estimate AGB on a plot basis it must have the complete number of trees per plot for precise AGB accounting. Table 4 show the number of trees per plot identified and extracted from the respective sensors.

Table 4. Trees identified and extracted by the respective sensor.

Plot No.	No. Trees Detected by Airborne LiDAR & Orthophoto	Extracted trees obtained from TLS	Total No. of Trees	Plot No.	No. Trees Detected by Airborne LiDAR & Orthophoto	Extracted trees obtained from TLS	Total No. of Trees
1	12	3	15	9	12	16	28
2	13	10	23	18	10	25	35
3	20	7	27	20	10	14	24
4	13	11	24	21	13	30	43
5	18	3	21	22	13	24	37
6	16	8	24	24	11	15	26
7	11	15	26	25	13	10	23
8	11	14	25	26	12	15	27
Sub-Total	**114**	**71**	**185**	**Sub-Total**	**94**	**149**	**243**

Total No. Trees Detected by Airborne LiDAR & Orthophoto	**208**
Total Extracted trees obtained from TLS	**220**
Total No. of Trees	**428**

3.5 Upper Canopy AGB calculation

3.5.1 CHM and CPA parameters

To assess the AGB for the upper canopy layer, DBH must was modelled using multiple regression. The two main parameters were required to model the DBH of this layer namely height and CPA. The generated CHM from Airborne LiDAR and CPA from the segmented Orthophoto were used to obtain a modelled DBH. This was applied because DBH cannot be measured directly from the images both from Airborne LiDAR and Orthophoto. Table 5 show the average CPA and height per plot. Figure 11 show the distribution and QQ plots of CPA and height.

Table 5. Average CPA and height per plot.

Plot No.	CPA	Height	Plot No.	CPA	Height
1	5.83	20.53	9	7.38	17.68
2	8.37	19.42	18	6.32	20.86
3	5.83	20.53	20	7.17	23.28
4	5.85	22.04	21	5.62	20.79
5	6.45	21.79	22	7.29	24.06
6	7.03	19.32	24	6.08	21.79
7	7.62	17.34	25	5.98	23.07
8	6.35	11.59	26	6.55	21.24

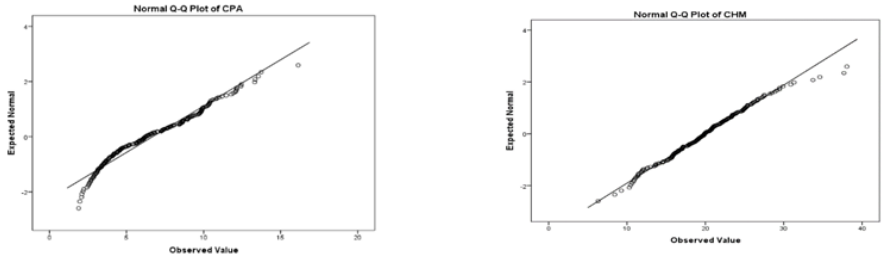

Figure11. Distribution and QQ plots of CPA and height.

3.5.2 DBH modelling using multiple regression analysis

Height generated from CHM and CPA from the segmented Orthophoto were used as independent variable and field measured DBH as the dependent variable to obtain a modelled DBH using multiple regression. The overall relationship between the modelled DBH and field measured DBH for the 16 plots is shown in Figure 12.

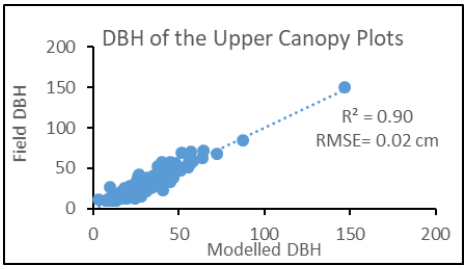

Figure12. Overall relationship between modelled and field DBH for the 16 plots.

Table 6 show the average modelled DBH and the average field measured DBH per plot. Figure 13 show the distribution and QQ plots of field and modelled DBH. Table 7 show the probability and reliability of the modelled and field measured DBH for the 16 plots.

Table 6. Average modelled and field DBH per plot.

Plot No.	Modelled DBH	Field DBH	Plot No.	Modelled DBH	Field DBH
1	23.91	23.92	9	29.70	29.92
2	38.63	38.62	18	34.30	34.33
3	29.28	29.30	20	38.00	38.00
4	30.68	30.69	21	27.35	27.54
5	30.67	30.67	22	27.77	27.77
6	24.54	24.56	24	36.72	36.73
7	20.18	20.18	25	27.70	27.85
8	20.28	20.09	26	24.88	24.33

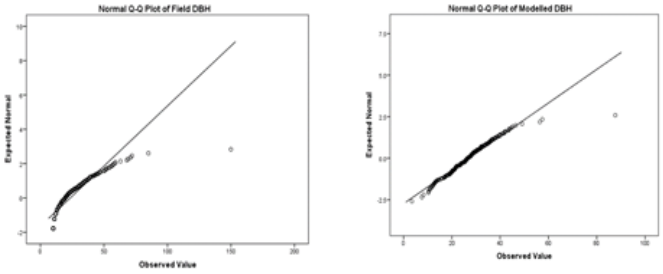

Figure13. Distribution and QQ plots of field and modelled DBH

Table 7. Regression statistics, probability and reliability of the modelled and field measured DBH for the 16 plots.

Regression Statistics		
R Square	Adjusted R^2	RMSE
0.90	0.89	0.02 cm

Regression probability and reliability				
	Coefficients		P-value	
Significance F	Intercept	Modelled DBH	Intercept	Modelled DBH
5.8E-105	-0.047	1.001	0.95	5.8E-105

The regression statistics of modelled DBH per plot is shown in Table 8. The regression probability and reliability of modelled DBH per plot is shown in Table 9

Table 8. Regression statistics of modelled DBH per plot.

Plot No.	R Square	Adjusted R Square	RMSE (cm)	Plot No.	R Square	Adjusted R Square	RMSE (cm)
1	0.93	0.91	3.13	9	0.91	0.89	4.52
2	0.97	0.96	6.82	18	0.95	0.94	4.76
3	0.89	0.87	5.56	20	0.88	0.84	8.61
4	0.78	0.74	5.97	21	0.86	0.83	4.80
5	0.85	0.84	6.97	22	0.89	0.87	4.28
6	0.75	0.71	5.08	24	0.76	0.70	8.31
7	0.89	0.86	2.48	25	0.80	0.75	8.50
8	0.79	0.74	4.76	26	0.81	0.77	6.22

Table 9. Regression statistics, probability and reliability of modelled DBH per plot.

		Coefficients			P-value		
Plot Number	Significance F	Intercept	CPA	Airborne LiDAR	Intercept	CPA	Airborne LiDAR
1	0.00054	-23.8318	3.44213	1.20555	0.02522	0.00045	0.00712
2	0.00000	-35.1645	-4.33123	5.66599	0.00057	0.00003	0.00000
3	0.00000	6.4450	-3.84735	2.20564	0.34477	0.00000	0.00000
4	0.00052	-36.2943	2.11197	2.47879	0.01150	0.00249	0.00042
5	0.00000	-70.6549	3.25972	3.68582	0.00001	0.00052	0.00000
6	0.00012	8.6789	-1.84090	1.49180	0.23153	0.00119	0.00039
7	0.00015	-3.2429	-0.93731	1.76242	0.43788	0.00322	0.00006
8	0.00194	5.3558	-2.04895	2.39355	0.42917	0.00452	0.00179
9	0.00002	9.3777	-2.53780	2.22004	0.15895	0.00041	0.00002
18	0.00002	-57.2368	3.46529	3.33836	0.00036	0.00030	0.00012
20	0.00069	-33.2824	-2.29377	3.76809	0.05461	0.01997	0.00033
21	0.00006	-32.9637	2.55242	2.21920	0.00197	0.00901	0.00008
22	0.00002	-53.4245	1.62452	2.88215	0.00016	0.00144	0.00001
24	0.00343	-35.7297	5.83201	1.69921	0.06259	0.00198	0.02333
25	0.00036	-28.6656	0.20537	2.39613	0.01390	0.85124	0.00021
26	0.00054	-23.8318	3.44213	1.20555	0.02522	0.00045	0.00712

3.5.3 Modelled AGB calculation and validation

AGB model for the upper canopy layer was calculated by applying the allometric equation by Chave et al., (2014). The values used in the equation are the modelled DBH and the height from the generated CHM. The modelled ABG was validated by applying the same allometric equation to the field measured DBH and height from the generated CHM. The modelled ABG was validated by applying the same allometric equation to the field measured DBH and height from CHM. Regression analysis between the modelled and field AGB was then conducted. Figure 13 show the overall relationship between the modelled and the field AGB for the 16 plots. Table 10 show the average AGB for the 16 plots.

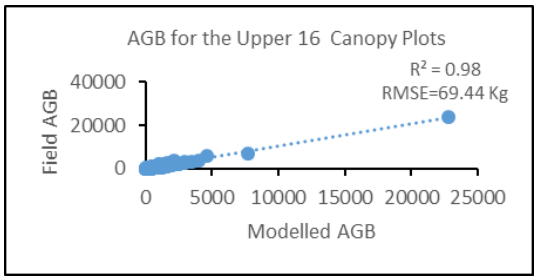

Figure 13. Overall relationship between the modelled and field measured AGB of the 16 upper canopy layer plots.

The regression statistics, probability and reliability of the modelled and field measured AGB for the 16 plots is shown in Table 11. The regression statistics of modelled and field AGB per plot is shown in Table 12. The regression probability and reliability of modelled AGB per plot is shown in Table 13.

Table 10. Average AGB for the 16 upper canopy plots.

Plot Number	Modelled AGB (kg/ plot)	Field AGB (kg/plot)	Plot Number	Modelled AGB (kg/plot)	Field AGB (kg/plot)
1	401	333	9	647	647
2	2324	2371	18	1055	1061
3	752	767	20	1495	1513
4	741	758	21	611	795
5	879	911	22	710	720
6	430	430	24	1027	1054
7	262	262	25	853	922
8	196	199	26	531	533

Table 11. Regression statistics, probability and reliability of the modelled and field measured AGB for the 16 plots.

Regression Statistics			Regression probability and reliability				
				Coefficients		P-value	
R Square	Adjusted R^2	RMSE	Significance F	Intercept	Modelled DBH	Intercept	Modelled DBH
0.98	0.98	69.44 Kg	1.8E-170	-3.88	1.03	0.86	1.8E-170

Table 12. Regression statistics of modelled and field AGB per plot.

Plot No.	Modelled AGB (kg/plot)	Field AGB (kg/ plot)	R^2	RMSE kg	Plot No.	Modelled AGB (kg/plot)	Field AGB (kg/ plot)	R^2	RMSE kg
1	4808	3991	0.95	68.67	9	7767	7928	0.95	147.07
2	30214	20827	0.99	171.90	18	10553	10609	0.95	249.05
3	15045	15348	0.95	200.20	20	14955	15131	0.96	425.53
4	9627	9855	0.75	309.73	21	7944	10332	0.93	221.29
5	15822	16396	0.84	451.30	22	9235	9365	0.88	250.34
6	6876	7075	0.77	175.49	24	11295	11597	0.72	454.81
7	2883	2920	0.91	68.95	25	11084	11987	0.95	334.71
8	2153	2192	0.94	65.21	26	6372	6401	0.74	366.95

Table 13. Regression probability and reliability of modelled AGB per plot.

		Coefficients		P-value	
Plot No.	Significance F	Intercept	Modelled AGB	Intercept	Modelled AGB
1	0.00000	30.91941	0.75296	0.31536	0.00000
2	0.00000	-55.00008	1.04394	0.30578	0.00000
3	0.00000	7.64259	1.00996	0.90065	0.00000
4	0.00012	-14.63952	1.04337	0.92789	0.00012
5	0.00000	-48.57211	1.09156	0.74684	0.00000
6	0.00001	4.95256	1.01741	0.94946	0.00001
7	0.00000	-14.23454	1.06701	0.69263	0.00000
8	0.00000	-12.80616	1.08357	0.64020	0.00000
9	0.00000	85.98751	0.88797	0.17574	0.00000
18	0.00000	87.24263	0.92265	0.43312	0.00000
20	0.00000	124.03345	0.92885	0.47356	0.00000
21	0.00000	23.82234	1.26157	0.78844	0.00000
22	0.00000	32.66846	0.96814	0.75245	0.00000
24	0.00081	-84.96709	1.10942	0.75905	0.00081
25	0.00000	-135.65397	1.24053	0.26571	0.00000
26	0.00032	-78.75753	1.15282	0.62391	0.00032

3.6 Lower Canopy AGB calculation

3.6.4 TLS acquired height and DBH and field measured DBH

Height and DBH are parameters measured directly from the extracted trees from the TLS. These parameters were used to model the AGB of trees in the lower canopy. The mean height and DBH from the extracted trees per plot as well as the field measured DBH are shown in Table 14.

Table 14. Mean height and DBH from trees extracted from TLS and mean field measured DBH.

Plot No.	TLS Height (m)	TLS DBH (cm)	Field DBH (cm)	Plot No.	TLS Height (m)	TLS DBH (cm)	Field DBH (cm)
1	9.87	16.53	16.70	18	14.69	18.84	19.00
2	13.75	13.26	14.00	20	14.65	19.43	19.43
3	14.60	19.39	22.00	21	15.55	17.87	17.80
4	15.36	20.15	20.18	22	15.58	16.79	16.79
5	14.33	22.47	23.67	24	15.53	18.52	19.20
6	14.80	12.64	12.75	25	16.26	16.85	17.00
7	15.15	22.35	22.33	26	13.86	17.37	17.40
8	8.64	19.89	20.00	18	14.69	18.84	19.00
9	12.95	16.79	16.81	20	14.65	19.43	19.43

The QQ plot distribution of the three parameters is shown in Figure 14.Table 15 show the regression statistics probability and reliability of the modelled and field measured DBH. Figure 15 show the graphical relationship between TLS and field DBH.

Figure 14. Distribution and QQ plot of TLS measured height and DBH and field DBH.

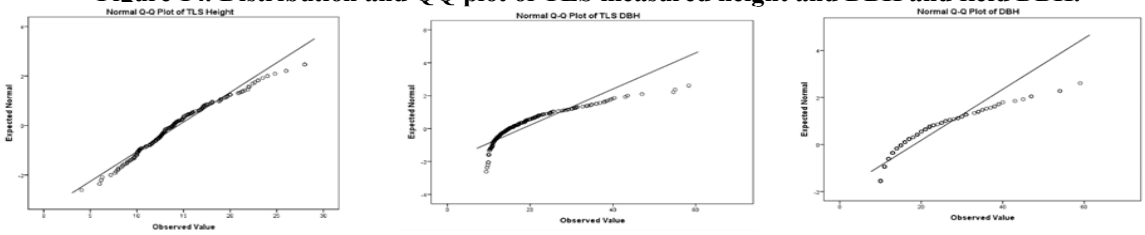

Table 15. Regression statistics, probability and reliability of the modelled and field measured DBH.

Regression Statistics	
R Square	RMSE
099	1.03 cm

Regression probability and reliability				
	Coefficients		P-value	
Significance F	Intercept	Modelled DBH	Intercept	Modelled DBH
3.9E-209	0.111	1.07	0.472	3.9E-209

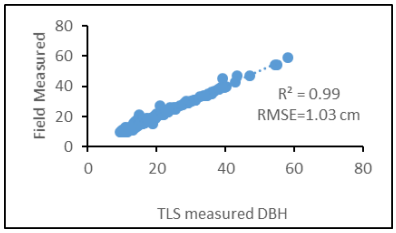

Figure 15. Relationship between TLS and field measured DBH.

3.6.5 AGB calculation and validation

The same allometric equation by Chave et al., (2014) was applied to calculate the AGB for the lower canopy. Calculating for the AGB used the TLS measured DBH and height parameters. The model was validated using the field DBH and TLS height. Regression analysis between the TLS modelled and field measured AGB was then conducted. Figure 16 show the overall relationship of the modelled and field AGB. Table 16 show the average AGB for the lower canopy plots. Table 17 show the regression statistics of the average calculated AGB for the lower canopy per plot. Plot level regression statistics of the modelled and field AGB is shown in Table 18.

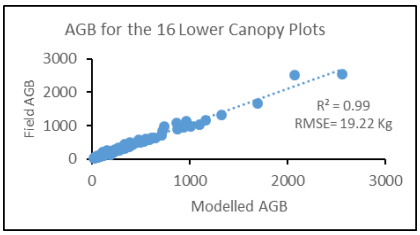

Figure 16. Overall relationship between the modelled and field AGB of the 16 lower canopy plots.

Table 16. Average AGB for the 16 lower canopy plots.

Plot. No.	Modelled AGB (KG/ plot)	Field AGB (KG/plot)	Plot. No.	Modelled AGB (KG/plot)	Field AGB (KG/plot)
1	96.04	97.84	9	148.48	149.28
2	83.11	96.59	18	242.40	243.10
3	209.85	273.94	20	251.31	251.31
4	242.40	243.87	21	242.22	291.59
5	364.46	417.11	22	195.13	193.31
6	100.01	102.26	24	307.36	307.36
7	346.11	345.89	25	208.14	206.91
8	135.30	136.25	26	171.90	173.03

Table 17. Regression statistics, probability and reliability of the modelled and field measured AGB for the 16 lower canopy plots.

Regression Statistics	
R Square	RMSE
0.99	19.23 kg

Regression probability and reliability				
	Coefficients		P-value	
Significance F	Intercept	Modelled DBH	Intercept	Modelled DBH
1.5E-205	-0.55	1.05	0.86	1.5E-205

Table 18. Plot level regression statistics of the modelled and field AGB

Plot No.	AGB TLS (kg /plot)	AGB Field (kg /plot)	R^2	RMSE (Kg)	Plot No.	AGB TLS (kg /plot)	AGB Field (kg /plot)	R^2	RMSE (Kg)
1	288	294	1	2	9	2376	2389	0.99	5.24
2	831	966	0.77	33.21	18	6060	6075	0.99	12.04
3	1469	1918	0.99	33.27	20	3518	3518	1	0
4	2666	2683	0.99	3.45	21	7267	8748	0.99	13.41
5	1093	1251	0.99	7.29	22	4683	4639	0.99	14.79
6	800	818	0.99	1.59	24	1640	4610	1	0
7	5192	5188	0.99	7.15	25	2081	2069	0.99	17.11
8	1894	1907	0.99	2.91	26	2579	2595	0.98	25.12

3.6.6 Summation of modelled AGB from upper and lower canopies

The overall modelled AGB was quantified by combining the validated values from both upper and lower canopies. The combined values are presented in Table 19.

Table 19. Summation of modelled AGB from upper and lower canopies.

Plot No.	AGB (Upper) (kg/ plot)	AGB (Lower) (kg/ plot)	Total Modelled AGB	Plot No.	AGB (Upper) (kg/plot)	AGB (Lower) (kg/plot)	Total Modelled AGB
1	4808	288	5096	9	7767	2376	10143
2	30214	831	31045	18	10553	6060	16613
3	15045	1469	16514	20	14955	3518	18473
4	9627	2666	12293	21	7944	7267	15211
5	15822	1093	16915	22	9235	4683	13918
6	6876	800	7676	24	11295	1640	12935
7	2883	5192	8075	25	11084	2081	13165
8	2153	1894	4047	26	6372	2579	8951

3.6.7 Summation of field AGB from upper and lower canopies

Likewise the overall field AGB from both upper and lower canopies were also combined. The combined values are presented in Table 20.

3.6.8 Accuracy assessment of the total modelled AGB

Accuracy of the combined modelled AGB was assessed by calculating the R^2 and RMSE. The graphical presentation of the accuracy of the combined upper and lower AGB is presented in Figure 16. The tabulated accuracy result for the respective upper and lower canopies are presented in Table 21. The accuracy of the combined modelled AGB is presented in Table 22.

Table 20. Summation of field AGB from upper and lower canopies.

Plot No.	AGB (Upper) (kg /plot)	AGB (Lower) (kg /plot)	Total Field AGB	Plot No.	AGB (Upper) (kg /plot)	AGB Field (Lower) (kg /plot)	Total Field AGB
1	3991	294	4285	9	7928	2389	10317
2	20827	966	21793	18	10609	6075	16684
3	15348	1918	17266	20	15131	3518	18649
4	9855	2683	12538	21	10332	8748	19080
5	16396	1251	17647	22	9365	4639	14004
6	7075	818	7893	24	11597	4610	16207
7	2920	5188	8108	25	11987	2069	14056
8	2192	1907	4099	26	6401	2595	8996

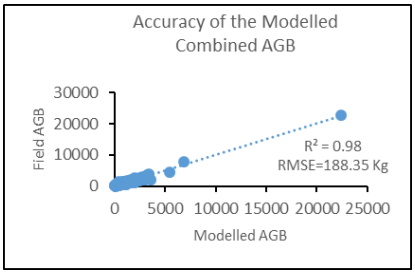

Figure 16. Accuracy of the combined upper and lower canopy modelled AGB.

Table 21. Accuracy of the modelled upper and lower AGB.

Plot No.	Total Modelled AGB (Kg/ plot)	R^2 Upper Canopy	R^2 Lower Canopy	RMSE Upper Canopy (Kg)	RMSE Lower Canopy (Kg)	Plot No.	Total Modelled AGB (Kg/plot)	R^2 Upper Canopy	R^2 Lower Canopy	RMSE Upper Canopy (Kg)	RMSE Lower Canopy (Kg)
1	5096	0.95	1	68.67	2.00	9	10143	0.95	0.99	147.07	5.24
2	31045	0.99	0.77	171.90	33.21	18	16613	0.95	0.99	249.05	12.04
3	16514	0.95	0.99	200.20	33.27	20	18473	0.96	1	425.53	0.00
4	12293	0.75	0.99	309.73	3.45	21	15211	0.93	0.99	221.29	13.41
5	16915	0.84	0.99	451.30	7.29	22	13918	0.88	0.99	250.34	14.79
6	7676	0.77	0.99	175.49	1.59	24	12935	0.72	1	454.81	0.00
7	8075	0.91	0.99	68.95	7.15	25	13165	0.95	0.99	334.71	17.11
8	4047	0.94	0.99	65.21	2.91	26	8951	0.74	0.98	366.95	25.12

Table 21. Accuracy of the combined modelled AGB.

Plot no	Total Modelled AGB (Kg/plot)	R^2	RMSE Kg	Plot no	Total Modelled AGB (Kg/plot)	R^2	RMSE Kg
1	5096.03	0.96	60.67	9	10142.22	0.96	96.94
2	31045.28	1.00	130.39	18	16613.15	0.97	126.53
3	12293.66	0.95	175.96	20	18473.23	0.97	261.82
4	16915.45	0.84	219.15	21	15211.01	0.97	117.41
5	7676.42	0.85	415.12	22	13917.83	0.93	141.36
6	8074.89	0.84	140.02	24	15905.61	0.88	280.63
7	4046.81	0.98	43.36	25	13165.34	0.96	250.91
8	10142.22	0.96	41.87	26	8950.68	0.79	234.30

4 Discussion

4.1 Data Distribution

The normality distribution of the field measured and sensor derived parameters were assessed because these parameters were needed for the subsequent regression analysis to derive AGB and carbon estimation. The distribution of the field measured DBH as showed in the result indicated a positive distribution to the right as well as the measured tree crown.

For the derived image parameter the distribution was symmetrical for the CHM and positively skewed to the right for the CPA. This symmetrical distribution of the CHM could be attributed to the identified trees from the image that are of taller heights except from the reforested area where trees of lower heights could be detected. In addition, taller trees have a greater chance of detection in airborne LiDAR because it has been proven to provide highly accurate height measurements due to higher point cloud densities near the sensor (Van Leeuwen et al., 2011). For the CPA it assumes a similar distribution pattern to the field measured crown which is positively skewed. This also implies that it has a similar distribution as the field measured DBH. As the result of King et al., (2005) who showed these parameters having a direct relationship therefore the CPA has shown similar variability as the field measured crown and DBH.

To test validity of the modelled and field DBH for subsequent AGB modelling the distribution was also tested. The distribution showed that it is positively skewed due to the one measurement which was extremely high. In this case it was included because the study is accounting for the accurate biomass on a plot basis. Excluding the tree would not reflect the substantial amount of biomass it has stored.

Testing the normality of TLS and field DBH distribution showed a positive skewness. This is because trees extracted from TLS reflect the same trees measured in the field. Thus, similarity in the pattern of distribution can be observed because trees above 10cm DBH were the ones measured. TLS height showed positive skewness because the trees extracted from the sensor are mostly of lower heights except for two trees which is way above the mean. As mentioned earlier for DBH extreme values were not excluded because estimation was based per plot and the substantial biomass stored of these trees must be accounted for.

4.2 Upper Canopy Layer

Calculating for the AGB of the upper canopy layer requires the generation of CHM from airborne LiDAR and CPA from the Orthophoto to produce a modelled DBH. DBH is one of the primary parameter required to calculate the AGB. Further, the accuracy of the modelled DBH is validated by the field measured DBH and the accuracy of the modelled AGB was validated by the field AGB. The succeeding sections discusses the obtained results.

Pit free CHM

Field measured height was not used due to data reliability. The presence of thick undergrowth causes occlusion upon tree height measurement. The occlusions in turn causes error readings using the instrument. Moreover, due to intermingling thick tree canopies measuring height underneath the forest is a challenge. Highest point of the tree is difficult to identify. Determining the highest point cause some biases for it is dependent on the handler of the instrument. Similar findings were observed in the studies by Andersen et al., (2006), O'Beirne, (2012)and Rönnholm et al., (2004).

Airborne LiDAR then was the only source for height data for estimating upper canopy AGB. Studies done by Lefsky et al., (2002) proved that LiDAR sensors can provide accurate and non-asymptotic estimates of various forest indices. As reviewed by Wulder et al., (2012) LiDAR sampling for large area forest characterization concluded that LiDAR can be treated as an independent measure to generate estimates of forest attributes for scientific studies. Thus, CHM was generated from 3D point cloud data from airborne LiDAR as done by Chen et al., (2005). However, the presence of "data pits" (irregularities in the surface canopy) reduced tree detection accuracy and subsequent biophysical measurements as observed by Ben-Arie et al., (2009). Producing pit free CHM was applied based on the study of Khosravipour et al., (2014) for it has been tested to produce better height measurements.

Segmentation accuracy

Application of multi-resolution segmentation was assessed in two ways. Measurement based on the segmented and referenced object was considered 1:1 if there was a 50% overlap (Zhan et al., 2005). The result of this study showed an accuracy of 77%. The results are comparable to studies done by Karna et al., (2013); Asmare, (2013) and Wang et al., (2004) that applied similar methods but of different type of forests. Further, over and under segmentation at the scale of 10 is 0.09 and 0.03 respectively with a D value of 0.25 (75%). Using fine scale value of 10 is considered most suitable to segment small objects like trees (Benz et al., 2004). The over and under segmentation values obtained can be considered the optimum fit for the upper canopy crowns. Higher over segmentation value compared to under segmentation indicate that automated segments exceed the area of the referenced polygons. This outcome is normal especially for complex and natural forests due to high variability in crown shape, multi-scale branching and tree clustering resulting to over segmentation (Jing et al., 2012).

4.3 Accuracy of the modelled DBH

The obtained R^2 value of the DBH for the 16 plots is 0.90 and RMSE of 0.02 cm. This indicate a strong relationship between height and CPA to model DBH as studied by Popescu, (2007). However, as compared to the result of Popescu, (2007) that obtained an R^2 of 0.87 and RMSE of 4.9 cm the values for this study obtained higher values. Higher values can be attributed through the direct processing of the airborne LiDAR data to derive height. The characteristic bias of using this method is measuring stand height towards the upper layers because the density of the point cloud is dependent on the last returns (Van Leeuwen et al., 2011).

Further, Maltamo et al., (2004) proved that using airborne LiDAR to obtain height revealed R^2 values ranging from 83 to 98%. For CPA segmentation using high resolution imagery yield better information for the upper canopy. Hirata et al., (2012) pointed out the impossibility to detect the middle and lower layers of a multi-layered forest. Related findings by Hou et al., (2011) for tropical forest application revealed that optical sensors can record mainly the tree crown surface while the understory will remain undetected.

4.4 Accuracy of the modelled AGB

AGB calculation for this study adopted the generic allometric equation of Chave et al., (2014). To calculate for AGB, height and DBH were the parameters used. LiDAR derived height is the only parameter used for all the calculations from AGB modelling and validation. This is due to reliability issues of the field measured height as previously discussed. Moreover, the accuracy of airborne LiDAR has been extensively studied (Lefsky et al., 2002; Popescu & Wynne, 2004) and proven to provide superior results for tropical forests (Hou et al., 2011; Tokola & Hou, 2012). It is the contention of this study that it is inappropriate to use data of low reliability for comparative purposes. Thus, it is not logical to compare data of known low reliability to the data which is proven to provide accurate results.

The calculated R^2 and RMSE for the 16 plots is 0.98 and 69.44 Kg respectively. To determine if the results are reasonable values it was compared to some related studies. Relevant studies that specifically deal with upper canopy estimation when the research was conducted was not found. Thus, it was compared with studies that estimate the overall estimation of specific area of the forest. It is relatively higher compared to the obtained values of Ediriweera et al., (2014) who obtained an R^2 of 0.83 for estimating biomass for subtropical and eucalypts forest. The result however is more comparable to the study of Karna et al., (2015) for reforested tropical forest in Nepal that obtained R^2 estimates ranging from 78-94% AGB. The high values obtained can be an indicator that the use of airborne LiDAR data as the standard height in combination with a high resolution imagery can produce robust results. This signifies the contention of Van Leeuwen et al., (2011) using LiDAR derived height can provide accurate results for its strength is towards the upper layers of the forest. Moreover, as pointed out by Hirata et al., (2012) high resolution imagery is well suited for measurement of upper crowns. In the overall assessment of AGB generally high R^2 values and low RMSE indicates good fit between the developed model and the sample plot (Lu, 2006).

4.5 Lower Canopy Layer

To obtain the overall biomass estimate of this multi layered forest it must be complemented with the measurements derived from the lower canopy. Using high resolution imagery is not possible because the middle and lower layers will not be observed (Hirata et al., 2012). As earlier discussed the bias of airborne laser signals is towards the upper layers and it becomes less towards the lower layers (Van Leeuwen et al., 2011). Thus, the use of TLS is applied to measure the structural parameters of the lower canopy. The derived parameters were then used to calculate for the lower canopy AGB.

Tree extraction

Multiple scanning technique was used to obtain full surface coverage of the tree. Registering the scanned positions aligned the scans to create a 3D perspective of the scene (Huang et al., 2010; Hopkinson, et al., 2004). This method further provide better scenes from the merged point cloud that can facilitate tree extraction (Liang, 2013 and Kankare et al., 2013).

Structural parameter measurement

Tree height is one of the main parameter measured from TLS to calculate the AGB for the lower canopy. Using the instrument is suited for this part of the study for its strength is towards the lower part of the canopy structure. Point cloud density increases as it becomes nearer to the sensor (Maas et al., 2008). In this case trees of lower height can be easily detected by the sensor. To note the measured height obtained is also not compared with field measured height. This is because studies on the use of TLS in forestry applications emphasized its potential use to substitute conventional field inventory (Lovell et al,. 2003; Bienert, et al., 2006 ; Lindberg, et al., 2012). Accuracy of the instrument could reach as high as 0.976 for correlations compared to manual measurements as studied by Rosell et al., (2009) or R^2 of 0.99 for stand parameter (Strahler et al., 2008).

Another parameter measured from TLS for AGB calculation is DBH. This was compared to the field measured DBH. The correlation result between the TLS and field measured DBH for this study showed an R^2 value of 0.99 and an RMSE of 1.03 cm. The RMSE result is slightly higher compared to the obtained values of Bienert et al., (2006) and Kankare et al., (2013) who obtained an RMSE of 1.5 cm and 1.48 cm respectively. This suggest that the obtained values of the two parameters have the potential to provide robust values for the estimation of the AGB.

AGB Accuracy

The same allometric equation by Chave et al., (2014) was used to estimate the lower canopy AGB. The calculated R^2 and RMSE for the 16 plots is 0.99 and 19.23 Kg respectively. The obtained R^2 value is higher and RMSE is lower compared to the study of Prasad, (2015) with an R^2 of 0.93 and RMSE of 42.4. It is also consistently higher compared to the study done by Kankare et al., (2013) that obtained an R^2 of 0.90 and 0.91 and RMSE of 22.12 kg and 26 kg respectively for Scots pine and Norway spruce.

The higher values can be attributed to the tested trees that come from the lower canopy only. For the previous studies it was applied to trees of varying heights. As indicated from the study of Prasad, (2015) high RMSE values indicate higher variability of measured tree height because most likely in their study both upper and lower canopies were assessed.

Accuracy of the combined modelled AGB

The combined AGB from the upper and lower canopies provided an overall estimate of the forest AGB. The obtained RMSEs for both canopy layers exhibited reasonable values. Calculating RMSEs indicate unbiased errors and follow a normal distribution (Chai and Draxler, 2014). Further, if there are more samples (eg. ≥100) reconstructing the error distribution using RMSE is more reliable. To support a very strong reliability of the modelled outcome more than 200 tree samples were used from each canopy layer. AGB values from the upper and lower canopy were combined as well as the R^2 and RMSE values. The obtained average R^2 and RMSE is 0.98 and 188.35 Kg respectively.

5. Conclusion

This study proposed an approach of assessing the AGB/carbon of a vertically complex structured tropical rain forest to obtain better accuracy. A complementary method of utilizing the strengths of airborne LiDAR and terrestrial laser scanning system is tested if this can provide accurate estimates of AGB/carbon of the different canopy layers of the forest. Estimating the AGB of the upper canopy layer made use of airborne LiDAR derived height and CPA from Orthophoto to derive a modelled of DBH through multiple regression. The achieved R^2 value of the modelled DBH for the 16 plots is 0.90 and RMSE of 0.02 cm. The modelled DBH together with LiDAR derived height was subsequently applied to the generic allometric equation to calculate for the modelled AGB and validated using the field measured DBH and LiDAR derived height. The result for the 16 plots achieved a model with an R^2 of 0.98 and RMSE of 69.44 Kg. To complement the AGB from the upper canopy the AGB of the lower canopy of the forest was assessed through the use of the TLS extracted trees that were not identified in the upper canopy layer. Using the derived measured parameters from the extracted trees, AGB of the lower canopy was calculated. The correlation of the TLS and field measured DBH was established and revealed an R^2 value of 0.99 and RMSE of 1.03 cm. The TLS height and DBH was then applied to the allometric equation and was used to derive the AGB of the lower canopy. Then the model was validated using the field measured DBH and TLS derived height. The achieved result was a model with an R^2 value of 0.99 and RMSE of 19.23 Kg for the 16 plots. The modelled AGB for the upper and lower canopies were then combined and further assessed for accuracy using R^2 and RMSE. The R^2 value achieved is 0.98 and the average RMSE is 188.35. The overall result showed some potential insights of utilizing remotely sensed data.

This study has provided some insights of the potential application of laser based and other remotely observed data to be used for rapid AGB/ carbon assessment in a tropical rain forest. In this study accuracy and reliability of the field height data was a challenging task to establish. Thus, obtaining the reasonable values rely heavily on the implementation of modelling techniques to achieve better accuracy assessments. This however suggests the greater potential of utilizing laser based height measurements for tropical rain forests. It is also recommended that further studies to be conducted will focus on the adoption of laser based methods of obtaining height and collect DBH metrics in the field for this type of forest to facilitate rapid AGB assessment..

Acknowledgements

This study was conducted in collaboration with ITC, University of Twente, Netherlands and University of Putra Malaysia. We would like to acknowledge Dr. Mohd Hasmadi Ismail, Mr. Farhan, Mohd Abdul Hafiz, Siti Zurina, Binti, Zakaria, Fazli Bin Shariff, Jelani Bin Alias, Noor Azlina Binti Azizdim, Mohd Fakhurallah bin Mohd Noh, Fazrul Azree Bin Mohd Arif by providing the logistical support in the field data collection. This work is funded through the University of Twente Excellence Scholarship Program and the University of the Philippines System Foreign Fellowship Program.

6. References

Aardt, J. a N. Van, Wynne, R. H., & Oderwald, R. G. (2004). A multi-resolution approach to forest segmentation as a precursor to estimation of volume and biomass by species. *Proceedings of the American Society for Photogrammetric Engineering and Remote Sensing Annual Conference*, 24–28. Retrieved from http://scholar.google.com/scholar?hl=en&btnG=Search&q=intitle:A+MULTI-RESOLUTION+APPROACH+TO+FOREST+SEGMENTATION+AS+A+PRECURSOR+TO+ESTIMATION+OF+VOLUME+AND+BIOMASS+BY+SPECIES#0

Andersen, H.-E., Reutebuch, S. E., & McGaughey, R. J. (2006). A rigorous assessment of tree height measurements obtained using airborne lidar and conventional field methods. *Canadian Journal of Remote Sensing*, *32*(5), 355–366. https://doi.org/10.5589/m06-030

Asmare, M. F. (2013). Airborne LiDAR data and VHR WORLDVIEW satellite imagery to support community based forest certification in Chitwan, Nepal, 1–78. Retrieved from http://www.itc.nl/library/papers_2013/msc/nrm/asmare.pdf

Ben-Arie, J. R., Hay, G. J., Powers, R. P., Castilla, G., & St-Onge, B. (2009). Development of a pit filling algorithm for LiDAR canopy height models. *Computers and Geosciences*, *35*(9), 1940–1949. https://doi.org/10.1016/j.cageo.2009.02.003

Benz, U. C., Hofmann, P., Willhauck, G., Lingenfelder, I., & Heynen, M. (2004). Multi-resolution, object-oriented fuzzy analysis of remote sensing data for GIS-ready information. *ISPRS Journal of Photogrammetry and Remote Sensing*, *58*(3–4), 239–258. https://doi.org/10.1016/j.isprsjprs.2003.10.002

Bienert, A., Maas, H., & Scheller, S. (2006). Analysis of the Information Content of Terrestrial Laserscanner Point Clouds for the Automatic Determination of Forest Inventory Parameters, 1–6.

Brown, S. (2002). Measuring carbon in forests: Current status and future challenges. *Environmental Pollution*, *116* (3), 363–372. https://doi.org/10.1016/S0269-7491(01)00212-3

Chai, T., Draxler, R. R., & Prediction, C. (2014). Root mean square error (RMSE) or mean absolute error (MAE)? – Arguments against avoiding RMSE in the literature, (2005), 1247–1250. https://doi.org/10.5194/gmd-7-1247-2014

Chave, J., R??jou-M??chain, M., B??rquez, A., Chidumayo, E., Colgan, M. S., Delitti, W. B. C., … Vieilledent, G. (2014). Improved allometric models to estimate the aboveground biomass of tropical trees. *Global Change Biology*, *20*(10), 3177–3190. https://doi.org/10.1111/gcb.12629

Chen, L., Chiang, T., & Teo, T. (n.d.). Fusion of LIDAR Data and High Resolution Images for Forest Canopy Modeling, (1), 3–9.

Clinton, N, Holt, A., Scarborough, J., Yan, L., & Gong, P. (2010). Accuracy assessment measures for object-based image segmentation goodness. *Photogrammetric Engineering & Remote Sensing*, *76*(3), 289–299. https://doi.org/10.14358/PERS.76.3.289

Clinton, Nicholas, Holt, A., Scarborough, J., Yan, L., & Gong, P. (2010). Accuracy {Assessment} {Measures} for {Object}-based {Image} {Segmentation} {Goodness}. *Photogrammetric Engineering & Remote Sensing*, *76*(3), 289–299. https://doi.org/10.14358/PERS.76.3.289

Corbera, E., & Schroeder, H. (2012). Governing and implementing REDD +. *Environmental Science and Policy*, *14*(2), 89–99. https://doi.org/10.1016/j.envsci.2010.11.002

Drăguţ, L., Tiede, D., & Levick, S. R. (2010). ESP: a tool to estimate scale parameter for multiresolution image segmentation of remotely sensed data. *International Journal of Geographical Information Science*, *24*(6), 859–871. https://doi.org/10.1080/13658810903174803

Drake, J. B., Knox, R. G., Dubayah, R. O., Clark, D. B., Condit, R., Blair, J. B., & Hofton, M. (2003). Above-ground biomass estimation in closed canopy Neotropical forests using lidar remote sensing: Factors affecting the generality of relationships. *Global Ecology and Biogeography*, *12*(2), 147–159. https://doi.org/10.1046/j.1466-822X.2003.00010.x

Ediriweera, S., Pathirana, S., Danaher, T., & Nichols, D. (2014). Estimating above-ground biomass by fusion of LiDAR and multispectral data in subtropical woody plant communities in topographically complex terrain in North-eastern Australia. *Journal of Forestry Research*, *25*(4), 761–771. https://doi.org/10.1007/s11676-014-0485-7

Emissions, R., & Management, S. (n.d.). REDD+ Cookbook 1.

Gibbs, H. K., Brown, S., Niles, J. O., & Foley, J. a. (2007). Monitoring and estimating tropical forest carbon stocks: making REDD a reality. *Environmental Research Letters*, *2*(4), 045023. https://doi.org/10.1088/1748-9326/2/4/045023

Hilker, T., van Leeuwen, M., Coops, N. C., Wulder, M. a., Newnham, G. J., Jupp, D. L. B., & Culvenor, D. S. (2010). Comparing canopy metrics derived from terrestrial and airborne laser scanning in a Douglas-fir dominated forest stand. *Trees - Structure and Function*, *24*(5), 819–832. https://doi.org/10.1007/s00468-010-0452-7

Hitam, A., Reserve, F., & M, W. R. W. (2014). COMMUNITY STRUCTURE OF TREES IN COMMUNITY STRUCTURE OF TREES IN AYER, (August 2015).

Hopkinson, C., Chasmer, L., Young-pow, C., & Treitz, P. (2004). Assessing forest metrics with a ground-based scanning lidar, *583*, 573–583. https://doi.org/10.1139/X03-225

Hou, Z., Xu, Q., & Tokola, T. (2011). ISPRS Journal of Photogrammetry and Remote Sensing Use of ALS , Airborne CIR and ALOS AVNIR-2 data for estimating tropical forest attributes in Lao PDR. *ISPRS JOURNAL OF PHOTOGRAMMETRY AND REMOTE SENSING*, *66*(6), 776–786. https://doi.org/10.1016/j.isprsjprs.2011.09.005

Huang, P., & Pretzsch, H. (2010). Using terrestrial laser scanner for estimating leaf areas of individual trees in a conifer forest, 609–619. https://doi.org/10.1007/s00468-010-0431-z

Hug, C., Ullrich, a, & Grimm, a. (2004). Litemapper-5600 – a waveform-digitizing LIDAR terrain and vegetation mapping system. *International Archives of Photogrammetry Remote Sensing and Spatial Information Sciences*, *XXXVI*, *PAR*, 24–29.

Ibrahim, F. (1999). Plant Diversity and Conservation Value of Ayer Hitam Forest, Selangor, Peninsular Malaysia. *Pertanika Journal of Tropical Agricultural Science*, *22*(2), 73–83.

Jing, L., Hu, B., Noland, T., & Li, J. (2012). ISPRS Journal of Photogrammetry and Remote Sensing An individual tree crown delineation method based on multi-scale segmentation of imagery. *ISPRS Journal of Photogrammetry and Remote Sensing*, *70*, 88–98. https://doi.org/10.1016/j.isprsjprs.2012.04.003

Kankare, V., Holopainen, M., Vastaranta, M., Puttonen, E., Yu, X., Hyyppä, J., … Alho, P. (2013). Individual tree biomass estimation using terrestrial laser scanning. *ISPRS Journal of Photogrammetry and Remote Sensing*, *75*, 64–75. https://doi.org/10.1016/j.isprsjprs.2012.10.003

Karna, Y. K., Hussin, Y. A., Gilani, H., Bronsveld, M. C., Murthy, M., Qamer, F. M., … Bhattarai, T. (2013). Integration of WorldView-2 and airborne LiDAR data for tree species level carbon stock mapping in Khayar Khola watershed, Nepal. *ISPRS Journal of Photogrammetry and Remote Sensing*, *In Review*, 280–291. https://doi.org/10.1016/j.jag.2015.01.011

Ketterings, Q. M., Coe, R., Van Noordwijk, M., Ambagau', Y., & Palm, C. a. (2001). Reducing uncertainty in the use of allometric biomass equations for predicting above-ground tree biomass in mixed secondary forests. *Forest Ecology and Management*, *146*(1–3), 199–209. https://doi.org/10.1016/S0378-1127(00)00460-6

Khosravipour, A. (2015). LiDAR point cloud processing Forestry LiDAR Derivatives CHM (Canopy Height Model), (November).

Khosravipour, A., Skidmore, A. K., Isenburg, M., Wang, T., & Hussin, Y. A. (2014). Generating Pit-free Canopy Height Models from Airborne Lidar, 863–872. https://doi.org/10.14358/PERS.80.9.863

Koch, B. (2010). Status and future of laser scanning, synthetic aperture radar and hyperspectral remote sensing data for forest biomass assessment. *ISPRS Journal of Photogrammetry and Remote Sensing*, *65*(6), 581–590. https://doi.org/10.1016/j.isprsjprs.2010.09.001

Lefsky, M. A., Cohen, W. B., Parker, G. G., & Harding, D. J. (2002). Lidar Remote Sensing for Ecosystem Studies, *52*(1), 19–30.

Liang, X. (2013). *Feasibility of Terrestrial Laser Scanning for Plotwise Forest Inventories*.

Lim, K., Treitz, P., Wulder, M., & Flood, M. (2003). LiDAR remote sensing of forest structure, *1*, 88–106.

Lindberg, E., Holmgren, J., Olofsson, K., Olsson, H., Lindberg, E., & Holmgren, J. (2012). Estimation of stem attributes using a combination of terrestrial and airborne laser scanning.

Lovell J.L. D.L.B.D.S. N.C. Coops Culvenor, A. (2003). Using airborne and ground-based ranging lidar to measure canopy structure in Australian forests. *Canadian Journal of Remote Sensing*, *29*(5), 607–622. https://doi.org/10.5589/m03-026

Lu, D. (2006). The potential and challenge of remote sensing-based biomass estimation. *International Journal of Remote Sensing*, *27*(7), 1297–1328. https://doi.org/10.1080/01431160500486732

Maas, H. -G. H.-G., Bienert, a., Scheller, S., & Keane, E. (2008). Automatic Forest Inventory Parameter Determination from Terrestrial Laser Scanner Data. *International Journal of Remote Sensing*, *29*(5), 1579–1593. https://doi.org/10.1080/01431160701736406

Majid S.A. and Narudin A.A. (2015). Aboveground biomass and carbon stock estimation in logged-over lowland tropical forest in malaysia, *1*(1978), 1–14.

Maltamo, M., Mustonen, K., Hyyppä, J., Pitkänen, J., & Yu, X. (2004). The accuracy of estimating individual tree variables with airborne laser scanning in a boreal nature reserve. *Canadian Journal of Forest Research*, *34* (9), 1791–1801. https://doi.org/10.1139/x04-055

Möller, M., Lymburner, L., & Volk, M. (2007). The comparison index: A tool for assessing the accuracy of image segmentation. *International Journal of Applied Earth Observation and Geoinformation*, *9*(3), 311–321. https://doi.org/10.1016/j.jag.2006.10.002

O'Beirne, D. (2012). Measuring the Urban Forest: Comparing Lidar Derived Tree Heights to Field Measurements.

Pistorius, T. (2012). From RED to REDD + : the evolution of a forest-based mitigation approach for developing countries. *Current Opinion in Environmental Sustainability*, *4*(6), 638–645. https://doi.org/10.1016/j.cosust.2012.07.002

Popescu, SC C, & Wynne, R. H. (2004). Seeing the trees in the forest: using lidar and multispectral data fusion with local filtering and variable window size for estimating tree height. *Photogrammetric Engineering & Remote …*, *70*(5), 589–604.

Popescu, Sorin C. (2007). Estimating biomass of individual pine trees using airborne lidar. *Biomass and Bioenergy*, *31*(9), 646–655. https://doi.org/10.1016/j.biombioe.2007.06.022

Prasad, O. M. P. (2015). Derivation of Forest Plot Inventory Parameters From Terrestrial Lidar Data for Carbon Estimation.

RIEGL. (2015). Riegl Vz-4000, 1–6.

Rönnholm, P., Hyyppä, J., Hyyppä, H., Haggrén, H., Yu, X., & Kaartinen, H. (2004). Calibration of laser-derived tree height estimates by means of photogrammetric techniques. *Scandinavian Journal of Forest Research*, *19*(6), 524–528. https://doi.org/10.1080/02827580410019436

Rosell, J. R., Llorens, J., Sanz, R., Arnó, J., Ribes-Dasi, M., Masip, J., … Palacín, J. (2009). Obtaining the three -dimensional structure of tree orchards from remote 2D terrestrial LIDAR scanning. *Agricultural and Forest Meteorology*, *149*(9), 1505–1515. https://doi.org/10.1016/j.agrformet.2009.04.008

Strahler, A. H., Jupp, D. L. B., Woodcock, C. E., Schaaf, C. B., Yao, T., Zhao, F., … Boykin-Morris, W. (2008). Retrieval of forest structural parameters using a ground-based lidar instrument (Echidna??). *Canadian Journal of Remote Sensing*, *34*(SUPPL. 2). https://doi.org/10.1007/s10342-010-0381-4

Suárez, J. C., Ontiveros, C., Smith, S., & Snape, S. (2005). Use of airborne LiDAR and aerial photography in the estimation of individual tree heights in forestry. *Computers and Geosciences*, *31*(2), 253–262. https://doi.org/10.1016/j.cageo.2004.09.015

Tokola, T., & Hou, Z. (2012). Alternative remote sensing materials and inventory strategies in tropical forest inventory - Case Lao PDR / Materiais alternativos de sensoriamento remoto e estratégias de inventário no inventário de florestas tropicais – Caso Lao PDR. *Revista Ambiência*, *8*(Especial), 483–500. https://doi.org/10.5777/ambiencia.2012.04.04

Tonolli, S., Dalponte, M., Neteler, M., Rodeghiero, M., Vescovo, L., & Gianelle, D. (2011). Fusion of airborne LiDAR and satellite multispectral data for the estimation of timber volume in the Southern Alps. *Remote Sensing of Environment*, *115*(10), 2486–2498. https://doi.org/10.1016/j.rse.2011.05.009

UN-REDD programme. (2015). The UN-REDD Programme Strategy.

Van Leeuwen, M., Hilker, T., Coops, N. C., Frazer, G., Wulder, M. a., Newnham, G. J., & Culvenor, D. S. (2011). Assessment of standing wood and fiber quality using ground and airborne laser scanning: A review. *Forest Ecology and Management*, *261*(9), 1467–1478. https://doi.org/10.1016/j.foreco.2011.01.032

Walter, H., Mueller-Dombois, D., & Burnett, J. H. (1973). Ecology of Tropical and Subtropical Vegetation. *The Geographical Journal*, *139*(2), 353. https://doi.org/10.2307/1796139

Wang, L., Gong, P., & Biging, G. S. (2004). Individual Tree-Crown Delineation and Treetop Detection in High-Spatial-Resolution Aerial Imagery. *Photogrammetric Engineering & Remote Sensing*, *70*(3), 351–357.

Watt, P. J., & Donoghue, D. N. M. (2005). Measuring Forest Structure with Terrestrial Laser Scanning. *Int J Remote Sens*, *26*(7), 1437–1446. https://doi.org/10.1080/01431160512331337961

Wulder, M. a., White, J. C., Nelson, R. F., Næsset, E., Ørka, H. O., Coops, N. C., … Gobakken, T. (2012). Lidar sampling for large-area forest characterization: A review. *Remote Sensing of Environment*, *121*, 196–209. https://doi.org/10.1016/j.rse.2012.02.001

Zhan, Q., Molenaar, M., Tempfli, K., & Shi, W. (2005). Quality assessment for geo-spatial objects derived from remotely sensed data. *International Journal of Remote Sensing*, *26*(14), 2953–2974. https://doi.org/10.1080/01431160500057764